Angular Distributions from Elastic Scattering of 15-MeV Deuterons*

R. K. Jolly, E. K. Lin, and B. L. Cohen
University of Pittsburgh, Pittsburgh, Pennsylvania
(Received 8 February 1963)

Angular distributions of 15-MeV deuterons elastically scattered by 23 elements between Al and Pb are presented. A high-resolution detection system provides complete separation from all inelastically scattered deuterons. In light and medium weight elements, there is a sharp diffraction pattern, but it damps out with increasing mass. In a few cases, there are marked differences between angular distributions from nuclei of nearly equal masses.

INTRODUCTION

In recent years, distorted-wave Born approximation calculations have been very successful in analyzing data on various types of direct nuclear reactions. The basic input data for these calculations are the optical model parameters, which are obtained from analyses of elastic scattering angular distributions. Since many of the most useful direct interactions involve deuterons [e.g., (d,p), (d,n), (d,t), (d,α), (d,Li^6), (p,d), (α,d), etc.], it is most important to have good data on elastic deuteron scattering over a range of energies.

A rather complete series of measurements of elastic deuteron scattering angular distributions at 11.8 MeV has been reported by Igo *et al.*,[1] and a few results have been reported at 13.0, 13.5, and 15.0 MeV by Cindro and Wall,[2] by the Cracow group,[3] and by Gofman *et al.*[4] at the Institute of Physics of the Academy of Sciences of the Ukrainian S.S.R. We here report a rather extensive study of this type with 15 MeV deuterons. In addition to being more extensive than previous studies, the present work utilizes better energy resolution than the previous work, which is important in some cases.

EXPERIMENTAL PROCEDURE AND ANALYSIS

The scattering facility used in conjunction with the University of Pittsburgh cyclotron has been described in detail previously[5]; it provides focusing and magnetic analysis of the incident deuteron beam, and magnetic analysis of the scattered particles. With its most recent modifications, a continuous range of angles from $-30°$ to $+140°$ may be studied, although measurements beyond 90° require a time consuming change of scattering chambers.

In the present experiment, the scattered particles are detected on the focal plane of the reaction product magnetic analyzing system by a triple scintillator apparatus shown in Fig. 1. It consists of three thin CsI (Tl) scintillation crystals, two 1/8-in.-wide "side" crystals on each side of the 1/4-in.-wide "center" crystal. In measuring the count rate of elastically scattered deuterons, the magnetic field is varied until practically all counts come from the center crystal and the count rates from the side crystals are equal; this assures that essentially all elastically scattered deuterons strike the center crystal, so that their intensity can be measured with a single magnet setting. It also provides sufficient energy resolution, ($\sim$150 keV) so that there can be no contribution from inelastic scattering even to first excited states for any of the nuclei studied. The detector is covered with sufficient absorber to eliminate tritons, and neither protons nor alpha particles have sufficient magnetic rigidity to reach the detector. In a few cases at back angles, the elastic peak was too wide to be detected by the center crystal only, so that corrections were applied using the count rate in the side crystals.

The incident deuteron energy cannot be carefully

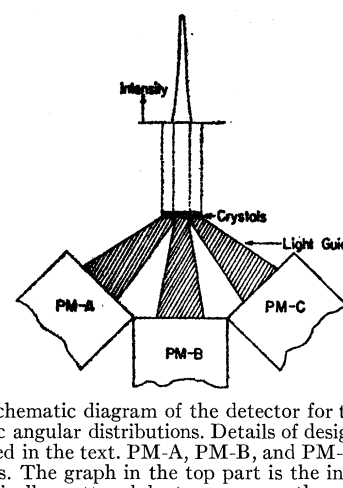

Fig. 1. Schematic diagram of the detector for the 15-MeV deuteron elastic angular distributions. Details of design and operation are explained in the text. PM-A, PM-B, and PM-C are photomultiplier tubes. The graph in the top part is the intensity distribution of elastically scattered deuterons across the crystals. By varying the analyzing magnetic field almost the entire elastic deuteron group could be made to fall on the center crystal as indicated in this figure.

* Work performed at Sarah Mellon Scaife Radiation Laboratory and supported by the National Science Foundation and the Office of Naval Research.

[1] G. Igo, W. Lorenz, and U. Schmidt Rohr, Report No. 29 (Max Planck Institute for Nuclear Physics, Heidelberg, Germany, 1961).

[2] Nikola Cindro and N. S. Wall, Phys. Rev. **119**, 1340 (1960).

[3] A. Buezanowski and K. Grotowski, Rept. No. 201 (Institute of Nuclear Physics, Cracow, 1962); A. Strzalkowski, Rept. No. 202 (Institute of Nuclear Physics, Cracow, 1962). L. Freindl, H. Nicwodniczanski, J. Nurzynski, M. Slapa, and A. Strzalkowski, Rept. No. 203 (Institute of Nuclear Physics, Cracow, 1962). H. Niewodniczanski, J. Nurzynski, and J. Wilczynski, Rept. No. 204 (Institute of Nuclear Physics, Cracow, 1962).

[4] Y. U. Gofman and O. F. Nemets, Zh. Eksperim. i Teor. Fiz. **39**, 1489 (1960) [translation: Soviet Phys.—JETP **12**, 1035 (1961)].

[5] R. S. Bender, E. M. Reilly, A. J. Allen, R. Ely, J. S. Arthur, and H. J. Hausmann, Rev. Sci. Instr. **23**, 542 (1952).

TABLE I. $(\sigma/\sigma_R)_{c.m.}$ vs $\theta_{c.m.}$ for 15-MeV deuterons elastically scattered from several elements.

Al $\theta_{c.m.}$	Al $(\sigma/\sigma_R)_{c.m.}$	Ti $\theta_{c.m.}$	Ti $(\sigma/\sigma_R)_{c.m.}$	Fe $\theta_{c.m.}$	Fe $(\sigma/\sigma_R)_{c.m.}$	Ni^{58} $\theta_{c.m.}$	Ni^{58} $(\sigma/\sigma_R)_{c.m.}$	Ni^{58} $\theta_{c.m.}$	Ni^{58} $(\sigma/\sigma_R)_{c.m.}$	Cu $\theta_{c.m.}$	Cu $(\sigma/\sigma_R)_{c.m.}$
21° 18′	0.920	19° 27′	0.771	19° 17′	0.735	20° 44′	0.723	94° 50′	0.138	20° 37′	0.734
23° 57′	0.799	22° 03′	0.665	21° 55′	0.686	23° 19′	0.578	97° 20′	0.122	23° 11′	0.689
26° 36′	0.560	24° 37′	0.497	23° 29′	0.481	25° 54′	0.477	99° 49′	0.0764	25° 45′	0.523
29° 12′	0.416	27° 21′	0.366	27° 03′	0.415	28° 29	0.386	102° 19′	0.0540	28° 19	0.482
31° 53′	0.311	29° 48′	0.275	29° 38′	0.335	31° 03	0.352	104° 48′	0.0498	30° 53	0.465
34° 31′	0.294	32° 23′	0.283	32° 22′	0.332	33° 37	0.397	107° 17′	0.0456	33° 27	0.454
37° 10′	0.413	34° 58′	0.377	34° 43′	0.424	36° 11	0.479	109° 45′	0.0449	36° 01	0.502
39° 47′	0.583	37° 33′	0.427	37° 31′	0.472	38° 46′	0.506	112° 13	0.0747	38° 35′	0.528
42° 25′	0.773	40° 08′	0.469	39° 53′	0.503	41° 20′	0.531	114° 40′	0.0948	41° 8′	0.490
45° 02′	0.915	42° 43′	0.497	42° 28′	0.508	43° 53′	0.507	117° 08′	0.0940	43° 41′	0.442
47° 39′	0.852	45° 16′	0.476	45° 01′	0.451	46° 27′	0.426	119° 36′	0.0955	46° 14′	0.345
50° 15′	0.679	47° 51′	0.427	47° 35′	0.360	49° 00′	0.349	122° 04′	0.0948	48° 47′	0.250
52° 51′	0.471	50° 24′	0.367	50° 07′	0.282	51° 33′	0.269	124° 31′	0.0905	51° 20′	0.190
55° 37′	0.314	52° 59′	0.342	52° 41′	0.248	54° 06′	0.218	127° 0′	0.0822	53° 53′	0.178
58° 02′	0.193	55° 31′	0.312	55° 13′	0.197	56° 39′	0.188	129° 25′	0.0731	56° 26′	0.184
60° 37′	0.165	58° 05′	0.318	57° 47′	0.209	59° 11′	0.195	131° 52′	0.0556	58° 58′	0.208
63° 12′	0.229	60° 37′	0.309	60° 15′	0.213	61° 43′	0.205	134° 19′	0.0449	61° 30′	0.246
65° 46′	0.367	63° 11′	0.295	62° 51′	0.218	64° 16′	0.218	136° 45′	0.0531	63° 32′	0.284
68° 20′	0.521	65° 43′	0.263	65° 23′	0.222	66° 48′	0.218	139° 11′	0.0465	66° 34′	0.260
70° 53′	0.680	68° 15′	0.220	67° 54′	0.219	69° 20′	0.225	141° 38	0.0432	68° 36′	0.251
73° 26′	0.803	70° 47′	0.162	70° 27′	0.199	71° 52′	0.218			71° 38′	0.242
75° 58′	0.848	73° 20′	0.121	72° 59′	0.196	74° 24′	0.219			73° 39′	0.221
78° 31′	0.800	75° 51′	0.124	75° 30′	0.192	76° 55′	0.220			76° 40′	0.188
81° 02′	0.704	78° 23′	0.139	78° 01′	0.195	79° 26′	0.218			78° 41′	0.162
83° 34′	0.600	80° 53′	0.176	80° 32′	0.202	81° 57′	0.210			81° 42′	0.146
86° 04′	0.467	83° 24′	0.230	83° 03′	0.206	84° 27′	0.193			83° 42′	0.135
88° 35′	0.356	85° 54′	0.284	85° 33′	0.196	86° 58′	0.170			86° 42′	0.114
91° 05′	0.265	88° 25′	0.321	88° 03′	0.180	89° 28′	0.157			88° 43′	0.113
93° 35′	0.197	90° 55′	0.331	90° 34′	0.170	92° 00′	0.130			91° 43′	0.100

Zn $\theta_{c.m.}$	Zn $(\sigma/\sigma_R)_{c.m.}$	Zr $\theta_{c.m.}$	Zr $(\sigma/\sigma_R)_{c.m.}$	Zr $\theta_{c.m.}$	Zr $(\sigma/\sigma_R)_{c.m.}$	Y $\theta_{c.m.}$	Y $(\sigma/\sigma_R)_{c.m.}$	Nb $\theta_{c.m.}$	Nb $(\sigma/\sigma_R)_{c.m.}$	Mo $\theta_{c.m.}$	Mo $(\sigma/\sigma_R)_{c.m.}$
20° 36′	0.707	20° 28′	0.905	94° 7′	0.160	20° 26′	0.800	19° 46′	0.851	19° 57′	0.926
23° 11′	0.660	23° 01′	0.840	96° 36′	0.149	22° 59′	0.787	22° 18′	0.825	22° 30′	0.855
25° 45′	0.486	25° 34′	0.696	99° 6′	0.098	25° 32′	0.692	24° 51′	0.740	25° 03′	0.731
28° 19	0.459	28° 07′	0.621	101° 36′	0.070	28° 05′	0.616	27° 24′	0.690	27° 36′	0.630
30° 53	0.440	30° 40′	0.562	104° 06′	0.058	30° 38′	0.551	29° 42′	0.566	30° 08′	0.553
33° 27	0.423	33° 16′	0.536	106° 35′	0.047	33° 11′	0.492	32° 29′	0.504	32° 41′	0.462
36° 01′	0.455	35° 46′	0.461	109° 04′	0.057	35° 44′	0.444	35° 03′	0.452	35° 14′	0.435
38° 35′	0.466	38° 19′	0.437	111° 33′	0.073	38° 17′	0.417	37° 36′	0.445	37° 44′	0.419
41° 8′	0.435	40° 51′	0.404	114° 02′	0.098	40° 49′	0.350	40° 08′	0.401	40° 18′	0.382
43° 41′	0.360	43° 24′	0.355	116° 31′	0.099	43° 22′	0.321	42° 41′	0.378	42° 51′	0.350
46° 14′	0.275	45° 56′	0.344	118° 59′	0.115	45° 54′	0.297	45° 13′	0.347	45° 23′	0.307
48° 47′	0.200	48° 28′	0.334	121° 27′	0.117	48° 26′	0.270	47° 46′	0.331	47° 55′	0.286
51° 20′	0.152	51° 0′	0.348	123° 55′	0.111	50° 58′	0.257	50° 18′	0.334	50° 26′	0.287
53° 53′	0.175	53° 32′	0.355	126° 23′	0.096	53° 30′	0.306	52° 50′	0.340	52° 58′	0.287
56° 26′	0.190	56° 04′	0.360	128° 51′	0.087	56° 02′	0.334	55° 22′	0.340	55° 30′	0.279
58° 58′	0.217	58° 35′	0.348	131° 19′	0.077	58° 33′	0.352	57° 54′	0.332	58° 02′	0.263
61° 30′	0.250	61° 07′	0.296	133° 47′	0.067	61° 05′	0.344	60° 25′	0.298	60° 33′	0.242
63° 32′	0.252	63° 39′	0.244	136° 15′	0.054	63° 36′	0.271	62° 57′	0.259	63° 04′	0.206
66° 34′	0.238	66° 10′	0.179	138° 43′	0.050	66° 07′	0.220	65° 29′	0.213	65° 35′	0.172
68° 36′	0.238	68° 42′	0.124	141° 10′	0.049	68° 39′	0.167	68° 00′	0.172	68° 07′	0.146
71° 38′	0.206	71° 13′	0.103			71° 11′	0.125	70° 31′	0.144	70° 38′	0.132
73° 39′	0.187	73° 44′	0.105			73° 41′	0.095	73° 02	0.136	73° 09′	0.134
76° 40′	0.154	76° 15′	0.123			76° 12′	0.101	75° 33′	0.147	75° 39′	0.130
78° 41′	0.133	78° 46′	0.150			78° 43′	0.124	78° 03′	0.165	78° 10′	0.154
81° 42′	0.122	81° 16′	0.191			81° 14′	0.143	80° 34′	0.191	80° 40′	0.165
83° 42′	0.102	83° 47′	0.210			83° 44′	0.198	83° 04′	0.205	83° 11′	0.169
86° 42′	0.105	86° 16′	0.221			86° 14′	0.216	85° 34′	0.210	85° 41′	0.165
88° 43′	0.097	88° 52′	0.203			88° 45′	0.216	88° 05′	0.206	88° 11′	0.154
91° 43′	0.089	91° 17′	0.189			91° 15′	0.204	90° 35′	0.190	90° 41′	0.148

TABLE I. $(\sigma/\sigma_R)_{c.m.}$ vs $\theta_{c.m.}$ for 15-MeV deuterons elastically scattered from several elements (*continued*).

Rh		Pd		Ag		Cd		In		Sn^{120}	
$\theta_{c.m.}$	$(\sigma/\sigma_R)_{c.m.}$	$\theta_{c.m.}$	$(\sigma/\sigma_R)_{c.m.}$	$\theta_{c.m.}$	$(\sigma/\sigma_R)_{c.m.}$	$\theta_{c.m.}$	$(\sigma/\sigma_R)_{c.m.}$	$\theta_{c.m.}$	$(\sigma/\sigma_R)_{c.m.}$	$\theta_{c.m.}$	$(\sigma/\sigma_R)_{c.m.}$
20° 15′	0.979	20° 14′	0.936	19° 40′	1.01	20° 22′	1.02	20° 04′	1.02	20° 22′	1.08
22° 48′	1.10	22° 47′	1.03	22° 13′	0.998	22° 53′	0.845	22° 35′	1.00	22° 54′	0.956
25° 21′	0.952	25° 19′	0.891	24° 46′	0.835	25° 26′	0.745	25° 08′	0.880	25° 27′	0.804
27° 54′	0.842	27° 51′	0.775	27° 18′	0.695	27° 58′	0.712	27° 40′	0.762	27° 59′	0.703
30° 26′	0.815	30° 23′	0.759	29° 50′	0.629	30° 30′	0.646	30° 12′	0.714	30° 31′	0.644
32° 59′	0.791	32° 56′	0.716	32° 22′	0.569	33° 02′	0.585	32° 44′	0.665	33° 03′	0.702
35° 31′	0.745	35° 28′	0.666	34° 55′	0.530	35° 35′	0.560	35° 17′	0.581	35° 35′	0.636
38° 04′	0.695	38° 00′	0.610	37° 27′	0.510	38° 07′	0.540	37° 49′	0.559	38° 07′	0.650
40° 36′	0.660	40° 32′	0.566	39° 59′	0.476	40° 39′	0.490	40° 21′	0.504	40° 39′	0.608
43° 08′	0.599	43° 04′	0.519	42° 31′	0.437	43° 11′	0.483	42° 53′	0.465	43° 11′	0.561
45° 40′	0.547	45° 36′	0.469	45° 03′	0.393	45° 43′	0.433	45° 25′	0.438	45° 43′	0.500
48° 12′	0.491	48° 08′	0.440	47° 35′	0.355	48° 15′	0.387	47° 57′	0.397	48° 15′	0.440
50° 44′	0.449	50° 39′	0.408	50° 07′	0.326	50° 47′	0.347	50° 29′	0.380	50° 46′	0.387
53° 16′	0.388	53° 11′	0.373	52° 39′	0.310	53° 19′	0.343	53° 01′	0.365	53° 19′	0.347
55° 48′	0.365	55° 42′	0.356	55° 10′	0.296	55° 50′	0.311	55° 32′	0.352	55° 49′	0.307
58° 20′	0.338	58° 14′	0.339	57° 41′	0.279	58° 31′	0.282	58° 03′	0.325	58° 21′	0.290
60° 51′	0.309	60° 45′	0.294	60° 13′	0.254	60° 53′	0.263	60° 35′	0.291	60° 52′	0.285
63° 22′	0.296	63° 17′	0.270	62° 45′	0.229	63° 25′	0.241	63° 07′	0.257	63° 22′	0.277
65° 53′	0.299	65° 48′	0.242	65° 16′	0.213	65° 56′	0.228	65° 48′	0.223	65° 54′	0.275
68° 25′	0.294	68° 19′	0.230	67° 47′	0.200	68° 27′	0.224	68° 09′	0.204	68° 25′	0.293
70° 56′	0.293	70° 50′	0.218	70° 18′	0.188	70° 58′	0.218	70° 40′	0.186	70° 56′	0.281
73° 27′	0.296	73° 21′	0.220	72° 49′	0.197	73° 29′	0.213	73° 11′	0.188	73° 26′	0.272
75° 58′	0.290	75° 52′	0.231	75° 20′	0.187	76° 00′	0.211	75° 42′	0.193	75° 57′	0.261
78° 29′	0.272	78° 23′	0.230	77° 50′	0.182	78° 30′	0.206	78° 12′	0.200	78° 27′	0.233
80° 59′	0.249	80° 53′	0.226	80° 20′	0.174	81° 00′	0.202	80° 42′	0.207	80° 58′	0.206
83° 29′	0.215	83° 24′	0.205	82° 50′	0.167	83° 30′	0.172	83° 12′	0.196	83° 28′	0.171
85° 59′	0.183	85° 54′	0.181	85° 21′	0.152	86° 01′	0.159	85° 43′	0.179	85° 59′	0.153
88° 29′	0.156	88° 24′	0.162	87° 51′	0.140	88° 31′	0.140	88° 13′	0.161	88° 28′	0.135
90° 59′	0.140	90° 54′	0.139	90° 21′	0.125	91° 01′	0.121	90° 43′	0.141	90° 59′	0.128
										93° 49′	0.127
										96° 19′	0.139
										98° 48′	0.138
										101° 18′	0.133
										103° 47′	0.130
										106° 17′	0.108
										108° 46′	0.083
										111° 16′	0.098
										113° 44′	...
										116° 13′	0.059
										118° 42′	0.065
										121° 11′	0.050
										123° 40′	0.050
										126° 09′	0.052
										128° 38′	0.058
										131° 06′	0.063
										133° 35′	0.062
										136° 03′	0.063
										138° 31′	0.065
										140° 59′	0.062

Er				Yb				Ta			
$\theta_{c.m.}$	$(\sigma/\sigma_R)_{c.m.}$	$\theta_{c.m.}$	$(\sigma/\sigma_R)_{c.m.}$	$\theta_{c.m.}$	$(\sigma/\sigma_R)_{c.m.}$	$\theta_{c.m.}$	$(\sigma/\sigma_R)_{c.m.}$	$\theta_{c.m.}$	$(\sigma/\sigma_R)_{c.m.}$	$\theta_{c.m.}$	$(\sigma/\sigma_R)_{c.m.}$
20° 14′	1.07	70° 38′	0.278	19° 37′	1.05	70° 01′	0.304	18° 57′	1.07	69° 19′	0.349
22° 46′	1.05	73° 09′	0.254	22° 09′	1.04	72° 32′	0.265	21° 29′	1.13	71° 50′	0.320
25° 17′	1.00	75° 39′	0.238	24° 40′	1.07	75° 02′	0.262	24° 00′	1.11	74° 20′	0.292
27° 49′	1.03	78° 10′	0.211	27° 12′	1.07	77° 33′	0.238	26° 32′	1.09	76° 51′	0.276
30° 20′	0.97	80° 40′	0.199	29° 43′	0.980	80° 03′	0.224	29° 03′	1.05	79° 21′	0.261
32° 51′	0.89	83° 10′	0.193	32° 14′	0.912	82° 33′	0.220	31° 34′	0.903	81° 52′	0.248
35° 23′	0.83	85° 40′	0.184	34° 46′	0.882	85° 03′	0.209	34° 06′	0.858	84° 22′	0.237
37° 54′	0.80	88° 10′	0.173	37° 17′	0.838	87° 33′	0.189	36° 37′	0.782	86° 53′	0.230
40° 26′	0.735	90° 40′	0.167	39° 49′	0.770	90° 03′	0.194	39° 08′	0.762	89° 23′	0.221
42° 57′	0.675			42° 20′	0.715			41° 40′	0.733		
45° 29′	0.577			44° 52′	0.635			44° 11′	0.649		
48° 00′	0.520			47° 23′	0.568			46° 42′	0.605		
50° 31′	0.463			49° 54′	0.517			49° 13′	0.577		
53° 02′	0.439			52° 25′	0.491			51° 45′	0.525		
55° 33′	0.414			54° 56′	0.441			54° 15′	0.499		
58° 04′	0.404			57° 27′	0.438			56° 46′	0.473		
60° 35′	0.370			59° 58′	0.428			59° 17′	0.453		
63° 06′	0.332			62° 29′	0.390			61° 48′	0.421		
65° 37′	0.326			65° 00′	0.387			64° 18′	0.407		
68° 08′	0.302			67° 31′	0.332			66° 49′	0.380		

TABLE I. $(\sigma/\sigma_R)_{c.m.}$ vs $\theta_{c.m.}$ for 15-MeV deuterons elastically scattered from several elements (*continued*).

W $\theta_{c.m.}$	W $(\sigma/\sigma_R)_{c.m.}$	Pt $\theta_{c.m.}$	Pt $(\sigma/\sigma_R)_{c.m.}$	Au $\theta_{c.m.}$	Au $(\sigma/\sigma_R)_{c.m.}$	Pb $\theta_{c.m.}$	Pb $(\sigma/\sigma_R)_{c.m.}$	Pb $\theta_{c.m.}$	Pb $(\sigma/\sigma_R)_{c.m.}$
20° 13′	1.10	18° 57′	1.00	20° 06′	1.00	18° 55′	1.00	91° 46′	0.195
22° 45′	1.07	21° 28′	1.05	22° 37′	1.00	21° 27′	1.10	94° 16′	0.259
25° 16′	1.04	23° 59′	1.03	25° 09′	1.03	23° 58′	1.10	96° 46′	0.242
27° 48′	1.08	26° 30′	1.06	27° 40′	1.02	26° 29′	1.15	99° 16′	0.208
30° 19′	1.03	29° 01′	1.04	30° 11′	1.00	29° 00′	1.12	101° 46′	0.202
32° 51′	0.951	31° 32′	1.02	32° 42′	0.948	31° 32′	1.02	104° 15′	0.160
35° 22′	0.957	34° 03′	0.919	35° 13′	0.917	34° 03′	0.970	106° 45′	0.127
37° 53′	0.891	36° 34′	0.842	37° 44′	0.862	36° 34′	0.990	109° 14′	0.148
40° 24′	0.836	39° 05′	0.828	40° 22′	0.828	39° 05′	0.944	111° 43′	0.124
42° 57′	0.801	41° 37′	0.789	42° 53′	0.801	41° 36′	0.904	114° 13′	0.094
45° 26′	0.747	44° 08′	0.738	45° 24′	0.741	44° 07′	0.869	116° 42′	0.113
47° 58′	0.656	46° 39′	0.686	47° 55′	0.705	46° 38′	0.806	119° 12′	0.105
50° 29′	0.614	49° 10′	0.658	50° 26′	0.665	49° 09′	0.779	121° 42′	0.068
53° 00′	0.554	51° 41′	0.601	52° 57′	0.663	51° 40′	0.703	124° 11′	0.068
55° 31′	0.529	54° 12′	0.564	55° 28′	0.601	54° 11′	0.671	126° 40′	0.073
58° 02′	0.511	56° 43′	0.524	57° 59′	0.505	56° 42′	0.584	129° 9′	0.068
60° 32′	0.456	59° 14′	0.474	60° 30′	0.458	59° 12′	0.534	131° 38′	0.069
63° 03′	0.414	61° 45′	0.452	63° 00′	0.436	61° 43′	0.503	134° 7′	0.068
65° 34′	0.398	64° 15′	0.425	65° 31′	0.405	64° 14′	0.493	136° 36′	0.065
68° 04′	0.384	66° 46′	0.411	68° 01′	0.381	66° 44′	0.489	139° 5′	0.063
70° 35′	0.348	69° 16′	0.384	70° 32′	0.377	69° 15′	0.448		
73° 05′	0.330	71° 47′	0.363	73° 02′	0.364	71° 45′	0.426		
75° 36′	0.292	74° 17′	0.340	75° 33′	0.331	74° 15′	0.410		
78° 06′	0.272	76° 48′	0.321	78° 03′	0.320	76° 46′	0.386		
80° 37′	0.257	79° 18′	0.301	80° 34′	0.304	79° 16′	0.346		
83° 07′	0.249	81° 49′	0.286	83° 04′	0.276	81° 46′	0.309		
85° 37′	0.231	84° 19′	0.256	85° 34′	0.247	84° 16′	0.246		
88° 08′	0.228	86° 49′	0.237	88° 04′	0.236	86° 46′	0.263		
90° 38′	0.218	89° 19′	0.229	90° 34′	0.212	89° 16′	0.254		

controlled, so that during the course of the experiments reported here it may have varied between 14.6 and 15.0 MeV. The variations during a measurement of a single angular distribution, however, are an order of magnitude smaller than this. Tests were made to ascertain that beam misalignment or scattering in the target do not cause errors in the Faraday cup beam current measurement even for the thickest and heaviest targets. The current integrator was frequently checked with a known current from a standard electrolytic cell.

Variations in target thickness (from the average value calculated from the total area and mass) was a particularly difficult problem in some cases; this was checked by use of several different targets of the same element.

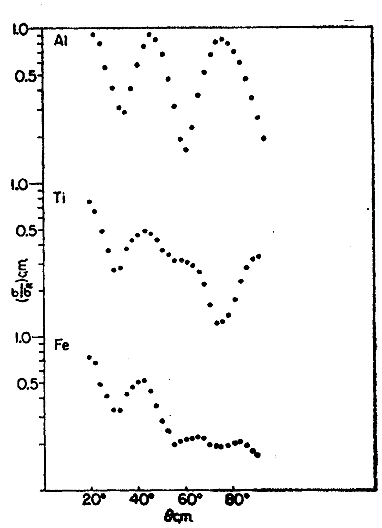

FIG. 2. Typical 15-MeV deuteron elastic scattering angular distribution data in the mass region $A=25$ to 60. Data points were taken at intervals of 2.5°. Ordinates are the ratios of total to Rutherford cross section at the scattering angles $\theta_{c.m.}$, which are the abscissas (in the center-of-mass system). Each point is the average of two or three independent experimental determinations. The scatter of the adjacent points tells the size of errors in the experiment.

The angle of the incident beam was checked frequently by measuring elastic scattering from a heavy element (target Au or Pt) at equal angles on each side of the nominal 0° and a zero angle correction was obtained from the intensity ratio between the two measurements by use of the Rutherford formula as follows: If the ratio of count rates at +20° and −20° (where these angles are measured from the nominal 0°) is R, the correction in degrees to the zero angle, Δ, is given by $\Delta=2.5(1-R)$. The zero angle varied from day to day by less than $\frac{1}{2}$ deg, and was uncertain by less than $\frac{1}{4}$ deg. The acceptance angle for scattered particles was usually 2°, but in some cases it was less. Errors in setting the scattering angle and in alignment were negligible. A detailed discussion of errors in experiments of this type has been given by Low.[6]

The most important errors due to angular uncertainties are eliminated by the method of determining absolute cross sections. This was done by normalizing all measurements to those for Pt at 20° and 25°, and assuming the Pt cross sections to be given correctly by the Rutherford formula at these small angles as is expected from optical model calculations. This method eliminates errors not only from angular uncertainties but from uncertainties in the geometry of the system

[6] C. A. Low, M.S. thesis, University of Pittsburgh, 1960 (unpublished).

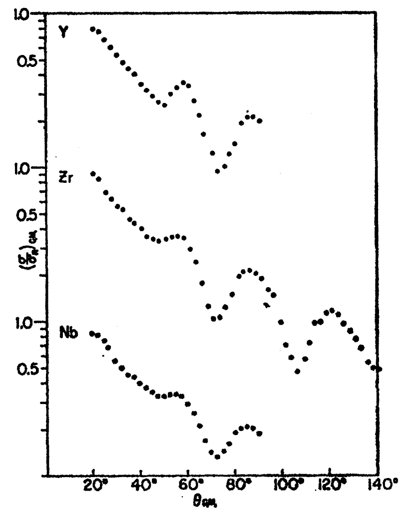

FIG. 3. Typical data in the mass region $A=85$ to 95. Zr data from 90 to 140° is the result of a single experiment. (See also caption for Fig. 2.)

arising from vertical bending by the fringe fields of the magnet.

Errors from imperfect performance of electronic instrumentation were checked by simultaneously feeding the signal from the center crystal into two different amplifier-discriminator-scalar systems. Results from the two systems were recorded in all runs. The scalars had 100 kC and 10 MC maximum count rates, respectively, so that errors due to excessive count rates were immediately detected. In all cases, count rates were kept conservatively low, but the lengths of runs were adjusted to give 1% statistical accuracy. Measurements were made at 2.5° intervals between 20° and 90° for all targets, and up to 140° for Ni, Zr, Sn^{120}, and Pb. All angular distributions were measured at least twice on separate days (many were done three or more times) and in no case was there a significant discrepancy in the shape of the angular distributions. There were discrepancies in the determinations of absolute cross sections, so that a large number of separate runs were made to check absolute cross sections at 20° and 25°. The discrepancies were found to be due to variations in thickness of the Au foils used for the early calibrations, so that Pt was used for calibrations in the later work.

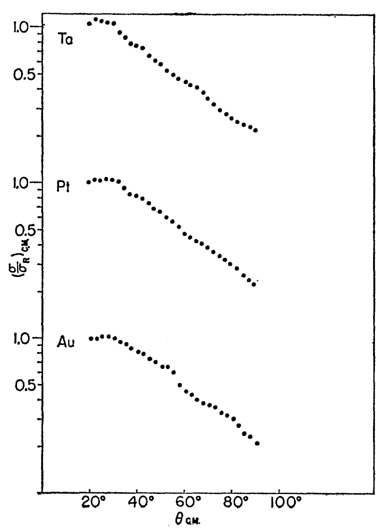

FIG. 4. Typical data in the mass region $A=180$ to 200. (See also caption for Fig. 2.)

RESULTS AND DISCUSSION

The values of $(\sigma/\sigma_R)_{c.m.}$ at different values of $\theta_{c.m.}$ for the different elements studied in the present work

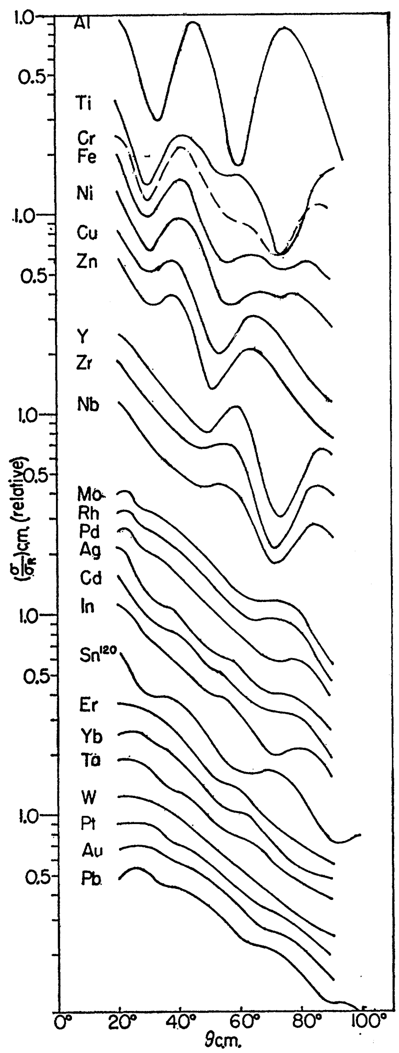

FIG. 5. Angular distribution of 15-MeV deuterons elastically scattered by 23 elements through the periodic table. The graphs are smooth curves drawn through the data points of Figs. 2–4 and five more similar figures and are displayed on a single diagram here for convenience of comparison of different angular distributions to study any systematic or singular variations in the structure of angular distributions with mass number A.

are given in Table I. Typical data picked from throughout the entire range of investigation are presented in Figs. 2–4. Figure 5 presents smooth curves drawn through the data points for all the elements and put together closely for studying the systematic and singular changes in structure as one goes through the periodic table. Such features as are immediately obvious from an examination of Fig. 5, are discussed below:

(1) (σ/σ_R) vs θ shows oscillations that are quite sharp in light nuclei but are increasingly damped as the mass increases. The oscillations are the well-known diffraction effect; their damping with increasing mass is well

known from other elastic scattering angular distribution experiments and can be explained by the volume absorption model[7] by changing the depth of the imaginary potential with nuclear mass, or by the surface absorption model[8] where it follows from the decrease in surface to volume ratio with mass.

(2) Maxima and minima of the distribution shift to smaller angles with increasing A as one expects from Fraunhofer diffraction theory, according to which[9]

$$(d\sigma/d\Omega)_{\text{Elastic}}=(Kr^2)^2[J_1(qr)/qr]^2, \qquad (1)$$

where J_1 is the first-order Bessel function, r is the interaction radius, K is the momentum of the incident particle, and q is the momentum transfer which, for elastic scattering, is

$$q=2K\sin(\theta/2). \qquad (2)$$

It is clear from (1) that the oscillations in the angular distributions arise from the Bessel function, so that the location of maxima and minima should depend only on the argument of the Bessel function, qr, which is proportional to $A^{1/3}\sin(\theta/2)$. To test this, the value of $A^{1/3}\sin(\theta/2)$ for each maximum and minimum in the angular distributions is plotted vs A in Fig. 6. According to the theoretical discussion above, the points in Fig. 6 lie along horizontal lines; this expectation is at least roughly fulfilled.

(3) Perhaps the most surprising feature of Fig. 5 is the few cases where there is a sharp change of angular distribution pattern over a small mass change. The most striking situation of this type is between Nb^{93} and Mo which has an average mass of 96. Another almost equally striking change is that between In^{115} and Sn^{120}. There are also striking differences between In^{115} and Cd (av $A=112$), between Rh^{103} and Pd (av $A=106$), and between Ni and Cu (av $A=59$ and 64, respectively). Such sharp changes are clearly contra-

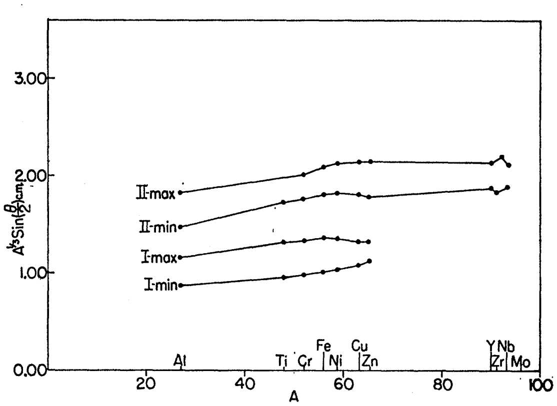

FIG. 6. Systematics of positions of maxima and minima from Fig. 5. The ordinate is $A^{1/3}\sin(\theta/2)$ and the abscissa is A, where θ is the scattering angle and A is the mass number of the scatterer.

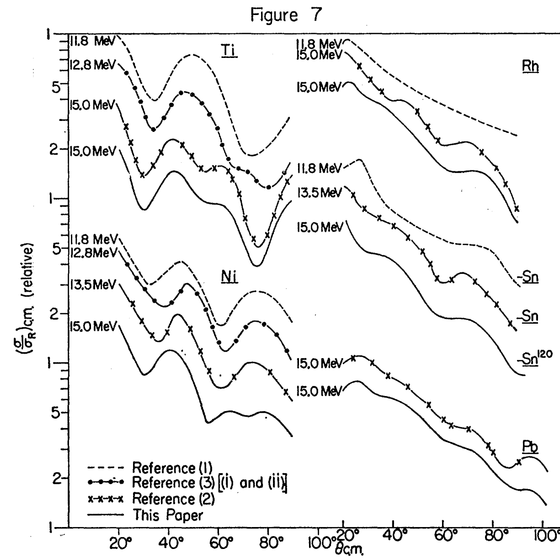

FIG. 7. The angular distributions of Ti, Ni, Rh, Sn, and Pb taken from the references indicated in the legend.

dictory to the basic assumptions of the optical model, and should be studied further.

(4) σ/σ_R averaged over the oscillations decreases with θ in all elements. The slope is mild in Al but gets large in medium and heavy elements though the change in slope is not very perceptible in the mass region $A=60$–200. Variations with mass in the aforesaid slope are much larger in (p,p)[10] and (α,α)[11] elastic scattering angular distributions.

A comparison with the 11.8 MeV data of Igo *et al.*[1] shows essential agreement with this data and the expected shift of peaks and valleys to smaller angles relative to their angular distributions. There are, however, discrepancies with the 15 MeV data of Cindro and Wall[2] in that the angular distributions for Rh and Pd, and for Cu and Fe are found to be similar in this work.

Some information on the energy dependence of elastic deuteron scattering is shown in Fig. 7, where data from references 1–3 are compared with this work. In general, the energy dependence is slowly varying, but there are a few nontrivial differences. For example, the minimum in the nickel angular distribution at ~70° does not appear at other energies.

An optical-model analysis of the data presented here is in progress.[12]

ACKNOWLEDGMENTS

The authors express their sincerest thanks to George Fodor for help in making targets and to John deFrancesco and Robert Leonard for help in facility operation and taking data.

[7] R. D. Woods and D. S. Saxon, Phys. Rev. **95**, 577 (1954).
[8] F. E. Bjorklund, S. Fernbach, and N. Sherman, Phys. Rev. **101**, 1832 (1956).
[9] See, for example, J. S. Blair, Phys. Rev. **115**, 928 (1959).
[10] B. L. Cohen and R. V. Neidigh, Phys. Rev. **93**, 282 (1954).
[11] I. S. Shapiro, Usp. Fiz. Nauk **75**, 61 (1961) [translation: Soviet Phys.—Usp. **4**, 674 (1962)].
[12] R. M. Drisko (private communication).